

## ภาคผนวก

### การวิเคราะห์หาความบริสุทธิ์ทางทฤษฎี

การวิเคราะห์หาความบริสุทธิ์ของสารประกอบอินทรีย์ โดยเทคนิค DSC ใช้พื้นฐานที่ว่า ปริมาณของสิ่งปลอมปนเพียงเล็กน้อย มีผลทำให้ช่วงของการหลอมที่กว้างขึ้น และอุณหภูมิของการหลอม ( $T_m$ ) ต่ำกว่าจุดหลอมของสารที่มีความบริสุทธิ์สูงมาก ๆ ( $T_0$ ) ดังนั้นถ้าสารมีสิ่งปลอมปนอยู่ในปริมาณที่แตกต่างกัน จะมีพีคของการหลอมและอุณหภูมิของการหลอมที่แตกต่างกันที่วิเคราะห์โดย DSC ที่แตกต่างกัน

ในการหาค่าเกี่ยวกับปริมาณสิ่งปลอมปนของสารอินทรีย์ จะพิจารณาจากพีคอุณหภูมิการหลอมเหลว ( $T_m$ ) และอุณหภูมิของการหลอมเหลว ( $\Delta H_m$ ) ที่ได้จาก DSC ซึ่งเป็นการตรวจวัดพลังงานที่ถูกดูดกลืนเข้าไปหรือถูกปลดปล่อยออกมาโดยสารตัวอย่าง ( $dq/dt$ ) โดยตรงซึ่งสามารถแสดงโดยสมการดังนี้

$$\frac{dq}{dt} = \frac{dT_s}{dt} \times \frac{dq}{dT_s} \quad (1)$$

เมื่อ  $\frac{dT_s}{dt}$  = อัตราเร็วของการตรวจวัด (scanning rate, degree/min)  
 $\frac{dq}{dT_s}$  = ความจุความร้อนของสารตัวอย่าง หรือพลังงานที่ต้องการเพื่อ ทำให้เกิดการเปลี่ยนแปลงความร้อน (joules/degree)

โดยเทอมความจุความร้อนของในสมการที่ 1 จะให้ข้อมูลที่มีความสำคัญเกี่ยวกับลักษณะของพีคของอุณหภูมิการหลอมของสารประกอบเป็นฟังก์ชันของอุณหภูมิของสาร จะทำให้ได้ความสัมพันธ์ของความร้อนที่ไหลเข้าไปยังสารตัวอย่างหรือความร้อนที่ไหลออกไปจากสารตัวอย่าง และการลดลงของจุดหลอมเหลวของสารตัวอย่างอันเนื่องมาจากการมีสิ่งปลอมปน โดยที่ความสัมพันธ์ดังกล่าวแสดงดัง สมการ 2 และ 3

$$\frac{dq}{dT_s} = \Delta q \frac{T_0 - T_m}{(T_0 - T_s)^2} \quad (2)$$

- เมื่อ  $\Delta q$  = ความร้อนทั้งหมดของการหลอมตัวของสารตัวอย่าง (joules)  
 $T_0$  = จุดหลอมเหลวของสารตัวอย่างที่มีความบริสุทธิ์ 100 %  
 $T_m$  = จุดหลอมเหลวของสารตัวอย่าง  
 $T_0 - T_m$  = การลดของจุดหลอมเหลวอันเนื่องมาจากสิ่งปลอมปน  
 $T_s$  = อุณหภูมิของสารตัวอย่าง

การลดของจุดหลอมเหลวอันเนื่องมาจากสิ่งปลอมปน ( $T_0 - T_m$ ) สามารถแสดงได้คือ

$$T_0 - T_m = \frac{RT_0^2 X_2}{\Delta H_m} \quad (3)$$

- เมื่อ  $R$  = ค่าคงที่ของก๊าซ (8.413 J/mol.K)  
 $X_2$  = สัดส่วนโมลของสิ่งแปลกปลอม  
 $\Delta H_m$  = ความร้อนของการหลอมเหลว (J/mol)

จากความสัมพันธ์พื้นฐานของ Van't Hoff (สมการ 2 และ 3) การหาความบริสุทธิ์ของสารในทางทฤษฎี โดย DSC สามารถทำได้โดยอินทิเกรต สมการ 2 ผลที่ได้แสดงถึงสัดส่วนของสารตัวอย่างที่มีการหลอมเหลวที่อุณหภูมิใดๆ บนเส้นกราฟของการหลอมเหลว ดังแสดงในสมการ 4 และ 5

$$F = \frac{T_0 - T_m}{T_0 - T_s} \quad (4)$$

จัดสมการ (4) ใหม่จะได้

$$T_s = T_0 - \frac{T_0 - T_m}{F} \quad (5)$$

- เมื่อ  $F$  = สัดส่วนการหลอม (fraction melted) ของสารตัวอย่าง  
 $T_s$  = อุณหภูมิของสารตัวอย่าง

แทนค่าสมการ (3) ในสมการ (5) จะได้สมการเส้นตรงสำหรับการหาความบริสุทธิ์โดย DSC ดังสมการ (6)

$$T_s = T_0 - \frac{RT_0^2 X_2}{\Delta H_m} \cdot \frac{1}{F} \quad (6)$$

เมื่อสมการ (6) เป็นสมการเส้นตรง การพล็อตระหว่างอุณหภูมิของสารตัวอย่าง ( $T_s$ ) กับส่วนกลับของการหลอมเหลวของสารตัวอย่าง ที่อุณหภูมินั้นๆ ( $1/F$ ) จะได้เส้นตรงที่มีความชันเท่ากับการลดลงของจุดหลอมตัว (ความชัน =  $RT_0^2 X_2 / \Delta H_m$ ) และจุดตัดบนแกน Y คือ  $T_0$

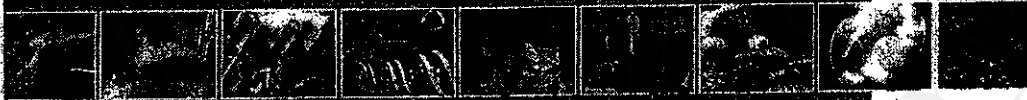
การพล็อตเส้นตรงนี้ เรียกว่า การพล็อตแบบ Van' t Hoff สัดส่วนของการหลอมของสารตัวอย่างที่อุณหภูมิต่างๆ สามารถหาได้โดยตรงจากโปรแกรมคอมพิวเตอร์ของเครื่อง DSC ซึ่งจะเป็นสัดส่วนกับพื้นที่ใต้พีคของเส้นกราฟที่อุณหภูมินั้นๆ โดยโปรแกรมคอมพิวเตอร์จะกำหนดช่วงที่ใช้การหาความบริสุทธิ์ของสารที่ใช้ในการวิเคราะห์ จากพีค  $T_m$  โดยแบ่งเป็นส่วนย่อย 20 ส่วนในช่วง 6-59 % ของการหลอม ทำให้สามารถคำนวณหาความบริสุทธิ์ของสารได้



# Abstracts บทคัดย่อ

## 32<sup>nd</sup> Congress on Science and Technology of Thailand (STT.32)

การประชุมวิชาการวิทยาศาสตร์และเทคโนโลยีแห่งประเทศไทย ครั้งที่ 32 (วทท.32)



To celebrate the 60<sup>th</sup> Anniversary  
of His Majesty the King's Accession to the Throne

เฉลิมฉลองการครองสิริราชสมบัติครบ 60 ปี  
ของพระบาทสมเด็จพระเจ้าอยู่หัว

Copyright © 2006  
โดย สภาส่งเสริมวิทยาศาสตร์และเทคโนโลยีแห่งประเทศไทย (สทท.)  
สงวนลิขสิทธิ์ 2547 สภาส่งเสริมวิทยาศาสตร์และเทคโนโลยีแห่งประเทศไทย

0001/STT.32/SOC OF TH

เชียงใหม่  
University

All rights reserved



Abstracts  
บทคัดย่อ  
32<sup>nd</sup> Congress  
on Science and Technology of Thailand (STT.32)  
การประชุมวิชาการวิทยาศาสตร์  
และเทคโนโลยีแห่งประเทศไทย ครั้งที่ 32 (วทท.32)

SCIENCE AND TECHNOLOGY FOR SUFFICIENCY ECONOMY  
To celebrate the 60<sup>th</sup> Anniversary  
of His Majesty the King's Accession to the Throne  
วิทยาศาสตร์และเทคโนโลยีเพื่อเศรษฐกิจพอเพียง  
เฉลิมฉลองการครองสิริราชสมบัติครบ 60 ปี  
ของพระบาทสมเด็จพระเจ้าอยู่หัว

October 10-12, 2006

Venue: QUEEN SIRIKIT NATIONAL CONVENTION CENTER (QSNCC)

10-12 ตุลาคม 2549

ณ ศูนย์ประชุมแห่งชาติสิริกิติ์



Organized by:

The Science Society of Thailand under the Patronage of His Majesty the King  
In association with Faculty of Science, Chulalongkorn University, Bangkok, Thailand

Supported by the National Research Council of Thailand

จัดโดย:

สมาคมวิทยาศาสตร์แห่งประเทศไทยในพระบรมราชูปถัมภ์  
ร่วมกับ คณะวิทยาศาสตร์ จุฬาลงกรณ์มหาวิทยาลัย

สนับสนุนโดย สำนักงานคณะกรรมการวิจัยแห่งชาติ

ลิขสิทธิ์ในภาพและข้อความสงวนลิขสิทธิ์  
Copyright © by Chiang Mai University  
All rights reserved



# EFFECTS OF HOT-DRAWING AND ANNEALING ON THE MECHANICAL PROPERTIES OF AN ABSORBABLE MONOFILAMENT SUTURE



Supap Bunkird, Jintana Siripitayananon, Robert Molloy, Rachanida Panjakha, Pajaree Chooprayoon.

Biomedical Polymers Technology Unit, Department of Chemistry, Faculty of Science Chiang Mai University, Chiang Mai 50200, Thailand

E-mail: [nitro\\_o@hotmail.com](mailto:nitro_o@hotmail.com) Tel: 053-943406 Fax: 053-892277

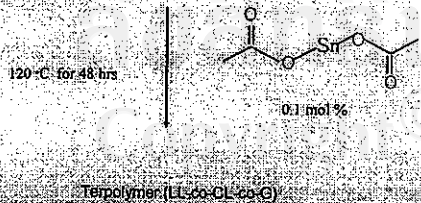
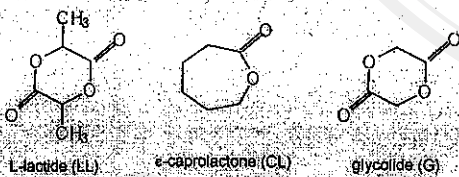
## ABSTRACT

A random terpolymer of L-lactide (LL), ε-caprolactone (CL) and glycolide (G) with a composition of 70:20:10 mol% was synthesized via bulk ring-opening polymerisation using stannous acetate as an initiator. The polymer was biodegradable with potential for use as an absorbable monofilament surgical suture. The polymer synthesized ( $M_w = 92300$ , from GPC) was spun into a monofilament fibre by a small-scale melt-spinning apparatus. The mechanical strength of the as-spun fibre was improved by off-line hot-drawing and annealing under controlled conditions of draw rate, draw ratio ( $\lambda$ ) and temperature. The results obtained from tensile testing showed that the fibre properties were strongly dependent on the draw ratio. A high draw ratio was obtained by off-line hot-drawing twice to  $\lambda = 6.44$  with intermediate annealing at 60 °C for 20 hrs. The tensile strength of the drawn fibre was found to increase by 1125 % relative to that of the as-spun fibre.

## Introduction

Terpolymers of L-lactide (LL), ε-caprolactone (CL) and glycolide (G) are biodegradable and biocompatible and have potential use as absorbable sutures. An appropriate balance of mechanical properties is essential for their use in this type of application. For example, the tensile strength of the fibre must be sufficiently high while, at the same time, maintaining sufficient flexibility for handling purpose. Such properties can only be achieved by controlling the polymer microstructure during synthesis and then by optimizing the conditions used in fibre processing. The aim of this study is to examine the effects of hot-drawing and annealing on the mechanical properties of the monofilament fibre during processing

## Synthesis and Characterization



Terpolymer	DSC			GPC	Intrinsic viscosity (dl g <sup>-1</sup> )
	T <sub>g</sub> (°C)	T <sub>m</sub> (°C)	ΔH <sub>m</sub> (Jg <sup>-1</sup> )	M <sub>w</sub>	
70:20:10	-	144	15.89	92300	0.595

Intrinsic viscosity measured in tetrahydrofuran (THF) at 40 °C

## Acknowledgements

We would like to thank the Department of Chemistry, Faculty of Science, Chiang Mai University and the National Metal and Materials Technology Center (MTEC).

## Fibre processing



Melt spinning was performed on pre-formed polymer rods which were melt-extruded through a single, circular hole spinneret with an exit diameter of 1.00 mm. The polymer was melted at 125 °C and extruded into a cooled water bath (5-10 °C) in order to obtain an almost amorphous as-spun fibre. The fibre dimensions were controlled by the extrusion rate and the take-up speed. The as-spun fibre was then drawn at 50 °C with a draw rate of 2700 % min<sup>-1</sup> followed by fixed-length annealing at 60 °C for 20 hrs in a vacuum. Finally, it was hot-drawn again at 60 °C to a total  $\lambda = 6.44$  using a maximum draw rate. In order to follow the changes induced in the fibre's matrix morphology, tensile testing of the fibre was carried out at each stage of processing

## Tensile testing

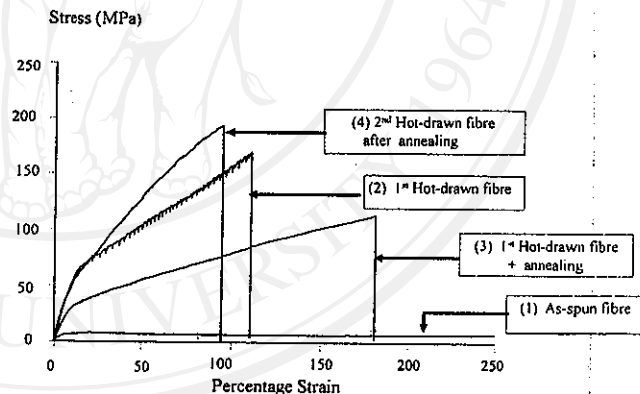


Fig.1 Comparison of the stress-strain curves for the fibre at various stages of its processing.

Tensile tests were performed at room temperature with a load cell = 100 N, initial gauge length = 40 mm and crosshead speed = 20 mm/min.

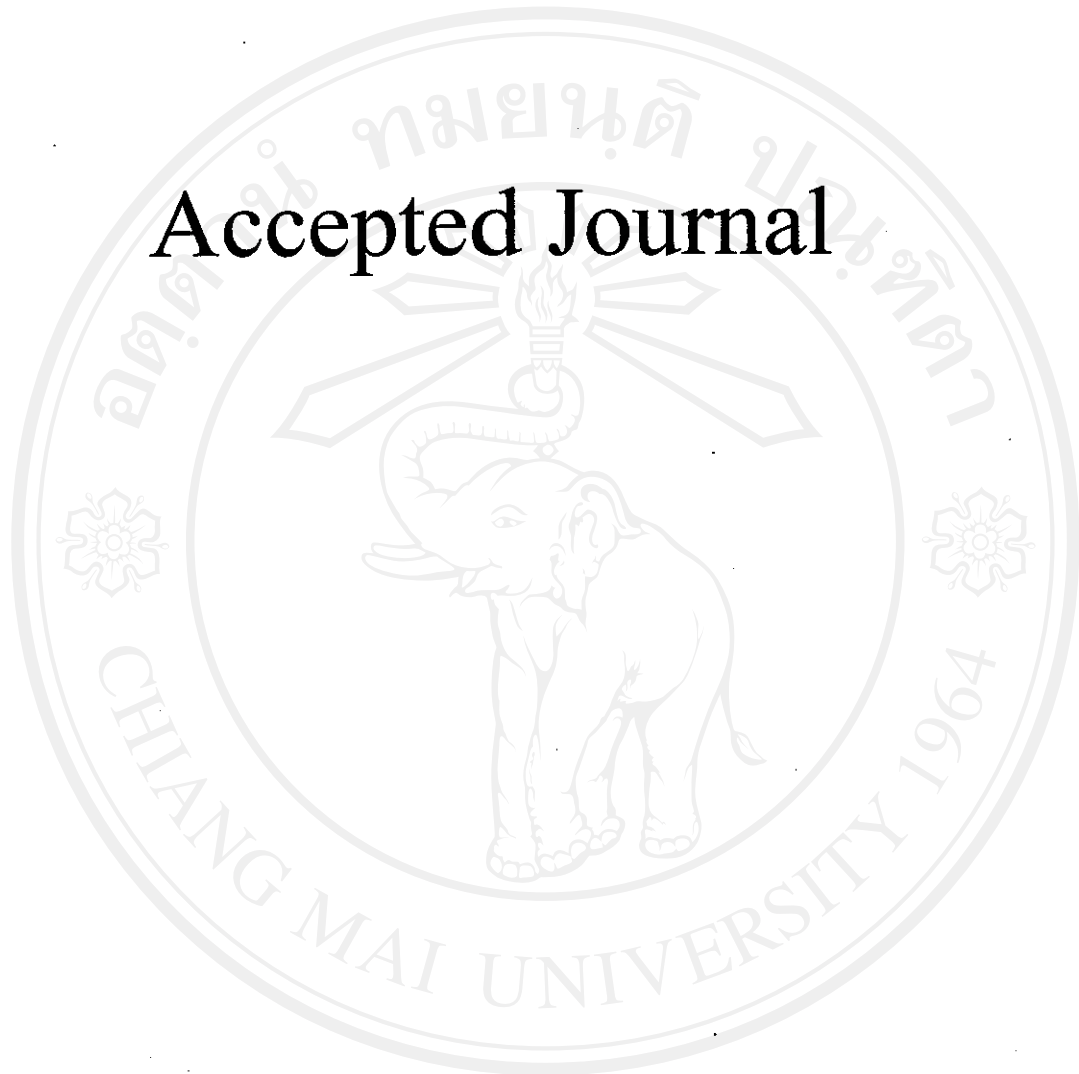
## Conclusions

The mechanical strength of the as-spun fibre was found to be dramatically improved by hot-drawing. Crystallisation after the 1<sup>st</sup> hot-drawing was induced by fixed-length annealing which also induced molecular relaxation leading to increased flexibility and elongation at break (see Fig.1). After the 2<sup>nd</sup> hot-drawing the molecular chains in both the amorphous and crystalline regions were forced to align along the fibre axis. As a result the fibre became stronger, as seen in Fig.1. These results show clearly the effects of hot-drawing and annealing. However, it is vitally important that the sequence of the operations and the temperature-time conditions employed be optimized in order to obtain the required balance of strength and flexibility. These studies are continuing as our understanding of the molecular orientation changes taking place is becoming clearer.

## References

1. Bezwa, R. S., Jamiolkowski, D. D., Lee, I. Y., Agarwal, V., Persivale, J., Benth, S., Emata, M., Suryadevara, J., Yang, A., and Lui, S., (1995) *Biomaterials* 16, 1141.
2. Ferguson, S., Wahi, D., and Gogolewski, S., (1995) *Biomaterials*, 17, 543.
3. Weiler, W., and Gogolewski, S., (1996) *Biomaterials*, 17, 529.

Accepted Journal



ลิขสิทธิ์มหาวิทยาลัยเชียงใหม่

Copyright© by Chiang Mai University

All rights reserved

# **Effects of Hot-drawing and Annealing on the Morphology and Mechanical Properties of Biodegradable Polyester Monofilament Fibers**

*J. Siripitayananon, R. Molloy<sup>\*</sup>, S. Bunkird, A. Kleawkla, R. Panjakha and P.  
Chooprayoon*

*Biomedical Polymers Technology Unit, Department of Chemistry, Faculty of Science, Chiang  
Mai University, Chiang Mai, Thailand*

ลิขสิทธิ์มหาวิทยาลัยเชียงใหม่

Copyright © by Chiang Mai University

<sup>\*</sup> Mail address: Dr. R. Molloy, Biomedical Polymers Technology Unit, Department of  
Chemistry, Faculty of Science, Chiang Mai University, Chiang Mai, Thailand 50200

E-mail: robert@chiangmai.ac.th



**ABSTRACT**

Co/terpolymers of L-lactide (LL),  $\epsilon$ -caprolactone (CL) and glycolide (G) are biodegradable in the human body and, as such, have considerable potential for use in biomedical applications such as absorbable surgical sutures, nerve guides, bone fixation devices and drug delivery systems. This study focuses its attention on their potential as monofilament fibers for absorbable suture applications. Random co/terpolymers with different compositions of LL, CL and G were synthesized via bulk ring-opening polymerization. The polymers obtained were melt spun at slow speeds into ice-cooled water to produce as-spun monofilament fibers with as little molecular orientation and crystallinity as possible. Combinations of off-line hot-drawing and annealing steps under controlled conditions of draw rate, draw ratio, temperature and time were then employed in order to develop the fiber's oriented semi-crystalline morphology. The mechanical properties of the fibers

were tested after each processing step and compared. The tensile test results showed that the tensile strength was strongly dependent on the draw ratio. A high draw ratio was obtained by multiple off-line hot-drawings with intermediate annealing. The first hot-drawing step dramatically enhanced the mechanical properties relative to those of the weak, highly extensible as-spun fiber. Subsequent annealing at a suitable temperature and for an appropriate length of time increased fiber flexibility as a result of molecular relaxation. Additional hot-drawing steps, again under precise temperature-time conditions, increased the total draw ratio and further enhanced the fiber's mechanical strength.

**Keywords :** Fibers; melt spinning; biodegradable polyesters; hot-drawing; annealing.

## 1 Introduction

Co/terpolymers of L-lactide (LL),  $\epsilon$ -caprolactone (CL) and glycolide (G) are known to be both biocompatible and biodegradable in the human body and so are widely used in biomedical applications such as absorbable surgical sutures (Baimark et al., 2005; Bezwada et al., 1995; Tomihata et al., 1998), absorbable nerve guides (den Dunnen et al., 1995; Meek et al. 1997; Rodriguez et al., 1999) and controlled-release drug delivery systems (Buntner et al., 1998; Ge et al., 2000; Pitt, 1990). Biodegradation proceeds via simple hydrolysis (random chain scission) leading to progressively lower molecular weight fragments which are then removed from the implant site by the body's own biological mechanisms. The added value of these materials lies in their versatility. By varying the co/terpolymer composition, monomer sequencing and molecular weight, the polymer properties can be specifically

tailored to meet the requirements of each particular application.

In this research work, attention is focused on absorbable monofilament surgical sutures. Absorbable surgical sutures can be classified into two main groups, namely: monofilaments and multifilaments. Monofilament sutures have a smooth surface and therefore show less tendency to harbor bacteria - major advantages in minimizing tissue drag and tissue reaction respectively. However, compared with multifilaments, they are relatively stiff and not so easy to handle. An appropriate balance of mechanical properties is therefore essential for their use in this type of application. For example, the tensile strength of the fiber must be sufficiently high while still maintaining sufficient flexibility for handling purposes. At the same time, the rate of biodegradation (hydrolysis) must be appropriate to the time required for absorption. The rationale for the choice of LL, CL and G as the three monomers is based upon these stringent property

requirements. LL is the main crystallizable component which determines the tensile strength. CL increases chain flexibility and thermal stability, thereby lowering the fiber stiffness and widening the melt processing window. Finally, G increases hydrophilicity and hydrolysability, thereby providing a means of adjusting the rate of biodegradation. By varying the composition, polymer properties can be tailored to meet specific demands.

However, such property control can only be achieved by (a) controlling the polymer's chemical microstructure during synthesis and then (b) by controlling the polymer's matrix morphology during fiber processing. The influence of the various synthesis parameters on copolymer microstructure has been well documented (Choi et al., 1994; Grijpma et al., 1991; Hiljanen-Vainio et al., 1996). The main aim of this present study is to examine the processing effects of hot-drawing and annealing on the morphology and mechanical properties of melt-spun P(LL-

co-CL) and P(LL-co-CL-co-G) monofilament fibers. Given the increasingly high cost of commercial absorbable monofilament sutures, these materials show potential for further development as lower-cost alternatives.

## 2 Materials and Characterization

Random co/terpolymers of L-lactide (LL),  $\epsilon$ -caprolactone (CL) and glycolide (G) with compositions of LL:CL:G = 75:25:0 and 70:20:10 mol % were synthesized via ring-opening polymerization in bulk using stannous acetate, Sn(Acet)<sub>2</sub>, as the initiator, as shown in Fig. 1. Precise details of the synthesis procedure used have been previously reported (Channuan et al., 2005). The mechanism of the polymerization reaction is of the so-called coordination-insertion type and has been described at length in the literature (Albertsson and Varma, 2003; Stridsberg et al., 2002). The polymer products obtained were rigorously purified by grinding into small pieces followed by

heating under vacuum at 100 °C to constant weight to remove any traces of residual monomer. Generally, polymer yields were near-quantitative (> 98 %) based on the initial combined monomer weights.

The co/terpolymer compositions and monomer sequence distributions were characterized using a Bruker Avance 1H/13C Nuclear Magnetic Resonance (NMR) Spectrometer. The compositions (mol %) from 1H-NMR are shown in Table 1 and corresponded with the initial monomer feed ratios. The monomer sequence distributions from 13C-NMR confirmed the random nature of the monomer sequencing but with some degree of blockiness which could be attributed to the differing monomer reactivities ( $G > LL > CL$ ). Weight-average molecular weights,  $M_w$ , were determined by gel permeation chromatography (GPC) using a Waters 717 Autosampler GPC and employing universal calibration (dual refractive index and viscosity detectors). Tetrahydrofuran (THF) was used as the solvent at 40 °C.

Intrinsic viscosities ( $[\eta]$ ) were determined by dilute-solution viscometry using a Schott-Geräte AVS300 Automatic Viscosity Measuring System, also employing THF as the solvent at 40 °C.

Thermal characterization was carried out by means of differential scanning calorimetry (DSC) and thermogravimetric analysis (TGA) using a Perkin-Elmer DSC7/TGA7 Thermal Analysis System at heating rates of 10 °C/min and 20 °C/min respectively. The melting peak parameters (peak  $T_m$  and heat of melting,  $\Delta H_m$ ) and thermal degradation temperatures ( $T_d$ ) are also shown in Table 1.

Despite their microstructural irregularity, the appearance of melting endotherms in the DSC thermograms of both the copolymer and terpolymer, as shown in Figs. 2(a) and 3(a), indicate that they were semi-crystalline in nature. However, their glass transition temperatures ( $T_g$ ) could not be clearly observed, as is often the case with crystallizable random copolymers. Instead, the  $T_g$  values given in parentheses

in Table 1 are estimates calculated from the Fox Equation (1) for a random co/terpolymer.

$$T_{gG} = 1 / \left( \frac{w_{LL}}{T_{gLL}} + \frac{w_{CL}}{T_{gCL}} + \frac{w_G}{T_{gG}} \right) \quad (1)$$

In Eq. 1,  $w_{LL}$ ,  $w_{CL}$  and  $w_G$  are the respective weight fractions of the LL, CL and G units, as calculated from the corresponding mole fractions  $m_{LL}$ ,  $m_{CL}$  and  $m_G$  from  $^1H$  NMR. Similarly,  $T_{gLL}$ ,  $T_{gCL}$  and  $T_{gG}$  are the respective  $T_g$  (K) values of the PLL ( $T_g = 65 \text{ }^\circ\text{C} = 338 \text{ K}$ ), PCL ( $T_g = -60 \text{ }^\circ\text{C} = 213 \text{ K}$ ) and PG ( $T_g = 35 \text{ }^\circ\text{C} = 308 \text{ K}$ ) homopolymers, as obtained from the reference literature (Perrin and English, 1997). When substituted into Eq. 1,  $T_g$  values for the P(LL-co-CL)75:25 copolymer and the P(LL-co-CL-co-G)70:20:10 terpolymer of 28  $^\circ\text{C}$  and 32  $^\circ\text{C}$  respectively are obtained. These values are consistent with the design criterion that these materials need to be flexible at room temperature.

Finally, the TGA curves for the co/terpolymers are compared in Fig. 4.

With initial thermal degradation (weight loss) temperatures ( $T_d$ ) of about 280  $^\circ\text{C}$ , the  $T_m$  and  $T_d$  values in Table 1 are sufficiently far apart ( $> 100 \text{ }^\circ\text{C}$ ) for thermal degradation during melt processing to be easily avoidable. As mentioned previously, the choice of CL as a comonomer is partly related to this question of melt stability. Not only are CL units more flexible than LL and G units, they are also more thermally stable. Hence, CL not only flexibilizes the polymer chain, it also improves its thermal stability, thereby widening the melt processing range. This is particularly relevant for producing absorbable surgical sutures where melt spinning is the preferred method of processing. Thermal degradation during processing is to be avoided at all costs since the resulting thermal degradation products (different from hydrolysis products) may be toxic to the human body.

### 3 Fibre Processing

The melt spinning apparatus used in this work was a modular-design, small-scale fiber extruder manufactured by Ventures & Consultancy Bradford Ltd. (formerly Bradford University Research Ltd.), Bradford, UK. A schematic arrangement of the apparatus is shown in Fig. 5 with a more detailed diagram of the compression, melting and metering zones, comprising the cylinder, heating block, filter mesh and spinnerette, shown in Fig. 6. The minimal dead volume within the system enabled sample sizes of as small as 20 g to be processed satisfactorily. The cooling bath (ice-cooled water) was maintained at a temperature of 5-10 °C, while the vertical distance (air gap) between the spinnerette (single circular hole, 1.0 mm diameter) and the surface of the bath liquid was kept constant at 4-5 cm.

Prior to melt spinning, the co/terpolymer chips were first compressed into cylindrical rods. This was done by heating the chips in the cylinder end-capped with a plain blanking plate under

pressure from the ram. Typically, a temperature within a range of about 10 °C either side of the initial (onset) melting temperature (from the DSC curve) was found to be suitable for this purpose, just enough for the chips to soften and stick together without appreciable melting. Melt spinning from these pre-formed rods gave fibers of more consistent quality than from chips and also reduced the tendency for void formation.

One of the prime considerations in any melt spinning process is the melt spinning temperature. This is because, for a given polymer molecular weight, the spinning temperature determines the melt viscosity which, together with the extrusion and take-up rates, determines the filament line stability. For the co/terpolymers studied here, it was found that a spinning temperature of peak  $T_m \pm 10$  °C (again from the DSC curve), depending on molecular weight, generally yielded fibers of consistent quality in terms of their uniformity of diameter and smooth surface appearance. As mentioned previously,

both of the co/terpolymers have wide melt processing ranges. Even so, it is preferable to choose a spinning temperature near the lower end of the range. This is because the higher the temperature, the more heat that needs to be dissipated from the extruded fiber as it cools. Hence, increasing the spinning temperature above the required minimum is only beneficial if it is really necessary to lower the melt viscosity.

In addition to the spinning temperature, the other main processing variables are the extrusion rate (ram speed), take-up rate, spinnerette diameter, the vertical distance (air gap) between the spinnerette and the cooling bath, and the cooling bath temperature. In combination, these variables control the as-spun fiber diameter at the macroscopic level and the degree of molecular orientation and crystallinity at the microscopic level. In this work, the intention was to produce as-spun fibers with as little molecular orientation and crystallinity as possible by employing slow extrusion rates coupled

with quench-cooling and just enough on-line drawing to maintain filament line stability. The rationale behind this was that it enabled the semi-crystalline morphology to be gradually built into the fiber through a succession of off-line hot-drawing and annealing steps under more controlled conditions. This multi-step approach also allowed for the fiber's morphology and mechanical property development to be followed at each step in the process. Off-line hot-drawing of the as-spun fibers was carried out at various temperatures within the range 40-80 °C at high draw rates of 2700-3800 %/min. Annealing (fixed length) was carried out at 60 °C for 20 hrs in a vacuum oven to allow molecular relaxation to occur.

The rod-forming and melt spinning temperatures, the extrusion and take-up rates, and the resultant as-spun fiber diameters are given in Table 2. The uniformity of the fiber diameters is notable bearing in mind that such slow spinning speeds were used. While slow speeds facilitate heat removal, they sometimes

give rise to an oscillatory instability known as “draw resonance”, the cause of which can be traced back to the tensile stress to which the extruded fiber is subjected. However, draw resonance was not encountered in this work within the range of spinning conditions studied, neither was cohesive or capillary fracture. The spinning dynamics were therefore considered to be conducive to the establishment of a stable and uniform filament line.

#### 4 Morphology Development

Recent work carried out in this research group has shown that random terpolymers of LL, CL and G containing 70 mol % or more of LL units exhibit a semi-crystalline morphology in which the crystalline component is essentially equivalent to the  $\alpha$  crystal phase of the PLL homopolymer (Channuan et al, 2005). Furthermore, the crystal structure appears to be largely invariant to different processing conditions, such as whether the terpolymer is crystallized under quiescent conditions

or hot-drawn from pre-spun fibers to a low or high draw ratio. Consequently, since the crystalline phase of these materials is similar to that of PLL, the following Eq. 2 can be used to calculate the % crystallinity to a reasonable approximation

$$\% \text{ Crystallinity} = (\Delta H_m \times 100) / \Delta H_m^* \% \quad (2)$$

where  $\Delta H_m$  is the heat of melting (from DSC) of the co/terpolymer and  $\Delta H_m^*$  is the heat of melting of a hypothetical 100 % crystalline sample of PLL (= 93.0 J/g) (Fischer et al., 1973).

As the appearance of melting peaks in their DSC curves in Figs. 2(a) and 3(a) shows, both the copolymer and the terpolymer were semi-crystalline materials as synthesized. Following their melt spinning, both of the co/terpolymer as-spun fibers were again semi-crystalline, as shown in Figs. 2(b) and 3(b), although with much reduced crystallinities as a result of quench-cooling. Subsequent hot-drawing then increased their crystallinities



back up again, as shown in Figs. 2(c) and 3(c), due to strain-induced crystallization resulting from enforced molecular alignment along the fiber axis. The % crystallinities at each of these three stages, as calculated using Eq. 2, are compared in Table 3.

## 5 Mechanical Properties

Mechanical (tensile) property testing was carried out using a Lloyds LRX+ Universal Testing Machine operating at room temperature under the following test conditions. Each fiber sample was tested at least five times before a test result was chosen which was considered to be truly representative of the sample.

grips = bollard-type
load cell = 100 N
initial gauge length = 40 mm
crosshead speed = 20 mm/min

The stress-strain curves for the P(LL-*co*-CL-*co*-G) terpolymer fiber after hot-drawing at various temperatures within the range 40-80 °C are shown in Fig. 7. This temperature range was chosen because it was immediately above the estimated glass transition temperature  $T_g$  of 32 °C (Table 1), thus allowing for a certain amount of molecular motion (chain segmental rotation) during hot-drawing. From the results in Fig. 7, the highest tensile strength (stress at break) was obtained for the fiber which was hot-drawn at 50 °C. Similar results were also obtained for the P(LL-*co*-LL) copolymer fiber. The stress-strain curves in Fig. 7 also demonstrate clearly how the mechanical strength of the as-spun fiber was dramatically improved by hot-drawing. As intended, the as-spun fiber, spun at a very low speed with quench-cooling and minimal on-line drawing, was basically a very weak, highly extensible fiber with low degrees of chain orientation and crystallinity. By design, these features were introduced into

the fiber's matrix by the subsequent hot-drawing process. The effects of hot-drawing on the thermal and tensile properties of the co/terpolymer fibers are demonstrated in Table 3.

## 6 Combined Effects of Hot-Drawing and Annealing

A single hot-drawing step at an appropriate temperature, as shown in the previous section, is clearly advantageous but is generally considered to be insufficient by itself to achieve the target properties. Instead, two or more hot-drawing steps are usually needed with intermediate annealing. Furthermore, rates of drawing, temperatures and times are all important variables which need to be studied and their influences understood. In this work, the overall fiber production process consisted of the following 4 stages. In between stages, the fibers were stored (at fixed length) at room temperature.

- (1) melt spinning (as-spun)
- (2) 1st hot-drawing at 50 °C
- (3) fixed-length annealing at 60 °C for 20 hrs
- (4) 2nd hot-drawing at 50 °C

The effects of these successive hot-drawing and annealing steps on the stress-strain curve are illustrated in Fig. 8 for the P(LL-co-CL-co-G) terpolymer fiber. Hot-drawing at 50 °C at fast drawing rates, as employed here, forces the molecules to align along the fiber axis against the constraints of molecular entanglements and with minimal time for molecular relaxation. This inevitably creates strain within the matrix. Fixed-length annealing at an appropriate temperature above  $T_g$ , in this case 60 °C, then allows the molecules to rearrange themselves into less-strained conformations but without accompanying fiber shrinkage. As seen in Fig. 8, this molecular relaxation has the combined effects of lowering both the tensile strength and initial modulus (stiffness). In the final stage (4), the 2nd hot-drawing step stretches the relaxed fiber, further

orienting the molecules in both the amorphous and crystalline phases, thereby increasing the tensile strength and modulus. A similar set of stress-strain curves to those shown in Fig. 8 was also obtained for the P(LL-co-CL) copolymer fiber.

## 7. Discussion and Conclusions

The melt spinning process which has been described here is a simple batch-type discontinuous process which is suitable for the small-scale production of speciality fibers but obviously not for the large-scale, high-speed production of commercial textile fibers. In such a highly specialized application as surgical sutures, the fiber's semi-crystalline morphology needs to be precisely controlled in order to be able to obtain the appropriate balance of physical, mechanical and biological properties, all of which are interrelated. Separating the processing steps is one way of achieving this level of control. It has been with this objective in mind that this work has focused its attention on studying the

effects of hot-drawing and annealing on the morphology and mechanical properties of the co/terpolymer fibers.

The mechanical property changes shown in Fig. 8 clearly demonstrate how an oriented semi-crystalline morphology can be gradually built into a fiber in a controlled way through a combination of hot-drawing and annealing steps. The mechanical strength of the as-spun fiber was dramatically improved by the 1st off-line hot-drawing as a consequence of the semi-crystalline morphology that was induced in the fiber matrix. The exact nature of this semi-crystalline morphology, both in terms of molecular orientation and degree of crystallinity, has profound effects on mechanical properties such as tensile strength and modulus. Due to the time-temperature dependency of solid-state molecular motion in polymers, an appropriate draw-rate at an appropriate temperature is essential for developing a morphology which gives properties suitable for a particular application. Furthermore, it is necessary to employ

annealing in order to stabilize the fiber morphology and facilitate molecular relaxation (Tsuji and Ikada, 1995). The main effects of annealing, as seen in Fig. 8, are to decrease the tensile strength but increase pliability and extensibility. The 2nd hot-drawing after annealing then restores the tensile strength. These findings are consistent with the generally accepted view that the higher the draw ratio, the stronger the fiber since the polymer chains in both the amorphous and crystalline regions are forced to align along the fiber axis (Fambri et al., 1997; Toki et al., 2002; Toki et al., 2003). However, in suture applications, tensile strength needs to be balanced with flexibility. The challenge therefore lies in finding the appropriate combinations of temperatures, rates and times necessary to obtain this balance.

In conclusion, these results have served to emphasize that both the melt spinning process and the post-spinning treatments are highly complex, multivariate procedures. Understanding

and controlling what the molecules are doing in response to the various forces being exerted upon them is the secret to success in obtaining fibers with the desired properties. This work has shown that, by performing the hot-drawing and annealing processes off-line rather than on-line, a greater level of molecular control can be achieved. These studies are continuing as our understanding of the molecular changes taking place is becoming clearer.

## References

- Albertsson, A-C., Varma, I.K., "Recent Developments in Ring-Opening Polymerization of Lactones for Biomedical Applications", *Biomacromolecules*, **4**, 1466-1486 (2003)
- Baimark, Y., Molloy, R., Molloy, N., Siripitayananon, J., Punyodom, W., "Synthesis, Characterization and Melt Spinning of a Block Copolymer of L-Lactide and  $\epsilon$ -Caprolactone for Potential Use as an Absorbable Monofilament Surgical Suture", *J. Mater. Sci.: Mater. Med.*, **16**, 699-707 (2005)
- Bezwada, R.S., Jamiolkowski, D.D., Lee, I-Y., Agarwal, V., Persivale, J., Trenka-Benthin, S., Erneta, M., Suryadevara, J., Yang, A., Liu, S., "Monocryl Suture, a New Ultra-pliable Absorbable Monofilament Suture", *Biomaterials*, **16**, 1141-1148 (1995)
- Buntner B., Nowak, M., Kasperczyk, J., Ryba, M., Grieb, P., Walski, M., Dobrzyński, P., Bero, M., "The Application of Microspheres from the Copolymers of Lactide and  $\epsilon$ -Caprolactone to the Controlled Release of Steroids", *J. Controlled Release*, **56**, 159-167 (1998)
- Channuan, W., Siripitayananon, J., Molloy, R., Sriyai, M., Davis, F.J., Mitchell, G.R., "The Structure of Crystallisable Copolymers of L-Lactide,  $\epsilon$ -Caprolactone and Glycolide", *Polymer*, **46**, 6411-6428 (2005)
- Choi, E.J., Park, J.K., Chang, H.N., "Effect of Polymerization Catalysts on the Microstructure of P(LLA-co- $\epsilon$ CL)", *J. Polym. Sci., Part B: Polym. Phys. Edn.*, **32**, 2481-2489 (1994)
- den Dunnan, W.F.A., van der Lei, B., Robinson, P.H., Holwerda, A., Pennings, A.J., Schakenraad, J.M., "Biological Performance of a Degradable Poly(lactic acid- $\epsilon$ -caprolactone) Nerve Guide: Influence of Tube Dimensions", *J. Biomed. Mater. Res.*, **29**, 757-766 (1995)
- Fambri, L., Pegoretti, A., Fenner, R., Incardona, S.D., Migliaresi, C., "Biodegradable Fibres of Poly(L-lactic acid) Produced by Melt Spinning", *Polymer*, **38**, 79-85 (1997)

Fischer, E.W., Sterzel, H.J., Wegner, G., "Investigation of the Structure of Solution Grown Crystals of Lactide Copolymers by Means of Chemical Reactions", *Colloid Polym. Sci.*, **251**, 980-990 (1973)

Ge, H., Hu, Y., Yang, S., Jiang, X., Yang, C., "Preparation, Characterization and Drug Release Behaviors of Drug-Loaded  $\epsilon$ -Caprolactone/L-Lactide Nanoparticles", *J. Appl. Polym. Sci.*, **75**, 874-882 (2000)

Grijpma, D.W., Pennings, A.J., "Polymerization Temperature Effects on the Properties of L-Lactide and  $\epsilon$ -Caprolactone Copolymers", *Polym. Bull.*, **25**, 335-341 (1991)

Hiljanen-Vainio, M., Karjalainen, T., Seppälä, J., "Biodegradable Lactone Copolymers. I: Characterisation and Mechanical Behaviour of  $\epsilon$ -Caprolactone and Lactide Copolymers", *J. Appl. Polym. Sci.*, **59**, 1281-1288 (1996)

Meek, M.F., den Dunnen, W.F.A., Bartels, H.L., Pennings, A.J., Robinson, P.H., Schakenraad, J.M., "Peripheral Nerve Regeneration and Functional Nerve Recovery after Reconstruction with a Thin-Walled Biodegradable Poly(DL-lactide- $\epsilon$ -caprolactone) Nerve Guide, *Cells Mater.*, **7**, 53-62 (1997)

Perrin, D.E., English, J.P., "Chapter 1: Polyglycolide and Polylactide", "Chapter 3: Polycaprolactone", in *Handbook of Biodegradable Polymers*, Domb, A.J., Kost, J., Wiseman, D.M. (Eds.), Harwood Academic Publishers, Amsterdam, p. 3-27, p. 63-77 (1997)

Pitt, C.G., "Chapter 3: Poly- $\epsilon$ -Caprolactone and its Copolymers", in *Biodegradable Polymers as Drug Delivery Systems*, Chasin, M., Langer, R. (Eds.), Marcel Dekker, Inc., New York, p. 71-120 (1990)

Rodriguez, F.J., Gomez, N., Perego, G., Navarro, X., "Highly Permeable Polylactide-Caprolactone Nerve Guides Enhance Peripheral Nerve Regeneration Through Long Gaps", *Biomaterials*, **20**, 1489-1500 (1999)

Stridsberg, K.M., Ryner, M., Albertsson, A-C., “Controlled Ring-Opening Polymerization: Polymers with Designed Macromolecular Architecture”, in *Degradable Aliphatic Polyesters*, Albertsson, A-C. (Ed.), Springer-Verlag, Berlin, *Adv. Polym. Sci.*, **157**, p. 41-65 (2002)

Toki, S., Sics, I., Ran, S., Liu, L., Hsiao, B., Murakami, S., Senoo, K., Kohjiya, S., “New Insights into Structural Development in Natural Rubber during Uniaxial Deformation by *In Situ* Synchrotron X-Ray Diffraction”, *Macromolecules*, **35**, 6578-6584 (2002)

Toki, S., Sics, I., Ran, S., Liu, L., Hsiao, B., “Molecular Orientation and Structural Development in Vulcanized Polyisoprene Rubbers during Uniaxial Deformation by *In Situ* Synchrotron X-Ray Diffraction”, *Polymer*, **44**, 6003-6011 (2003)

Tomihata, K., Suzuki, M., Oka, T., Ikada, Y., “A New Resorbable Monofilament Suture”, *Polym. Degrad. Stab.*, **59**, 13-18 (1998)

Tsuji, H., Ikada, Y., “Properties and Morphologies of Poly(L-lactide): 1. Annealing Condition Effects on Properties and Morphologies of Poly(L-lactide)”, *Polymer*, **36**, 2709-2716 (1995)

### Acknowledgements

Financial support for this work was provided by the National Metal and Materials Technology Center (MTEC), Thailand. The authors also wish to thank the Department of Chemistry, Faculty of Science, Chiang Mai University, Thailand, for provision of the research facilities.

ลิขสิทธิ์มหาวิทยาลัยเชียงใหม่

Copyright© by Chiang Mai University

All rights reserved

Co/terpolymer composition LL : CL : G <sup>a</sup> mol %	GPC	Viscometry	DSC			TGA
	M <sub>w</sub> <sup>b</sup>	[η] <sup>c</sup> dl/g	T <sub>g</sub> <sup>d</sup> °C	T <sub>m</sub> <sup>e</sup> °C	ΔH <sub>m</sub> <sup>f</sup> J/g	T <sub>d</sub> <sup>g</sup> °C
Co 75 : 25 : 0	8.37 x 10 <sup>4</sup>	0.587	(28)	155	19.4	280
Ter 70 : 20 : 10	9.23 x 10 <sup>4</sup>	0.595	(32)	151	22.3	280

<sup>a</sup> as determined from <sup>1</sup>H-NMR peak integrations

<sup>b</sup> using THF as solvent at 40 °C (universal calibration)

<sup>c</sup> using THF as solvent at 40 °C

<sup>d</sup> as calculated from the Fox Equation (Eq. 1)

<sup>e</sup> peak T<sub>m</sub> from melting endotherm

<sup>f</sup> heat of melting ∝ T<sub>m</sub> peak area

<sup>g</sup> initial weight loss temperature

Table 1. Molecular weight and thermal property characterization of the P(LL-co-CL) 75:25 copolymer and the P(LL-co-CL-co-G) 70:20:10 terpolymer as obtained from synthesis.

Co/terpolymer Sample	Rod-forming temperature °C	Melt spinning temperature °C	Extrusion rate m/min	Take-up rate m/min	On-line draw ratio	As-spun fiber diameter mm
P(LL-co-CL)	135	155	0.12	0.50	4.2	0.90 ± 0.02
P(LL-co-CL-co-G)	130	145	0.12	0.50	4.2	0.76 ± 0.02

Table 2. Processing conditions used for producing the as-spun co/terpolymer fibers

(spinnerette diameter = 1.0 mm).



Co/terpolymer Sample	Peak T <sub>m</sub> °C	ΔH <sub>m</sub> J/g	Crystallinity <sup>a</sup> %	Fiber diameter mm	Draw ratio	Stress at break MPa	% Strain at break %
<u>P(LL-co-CL)</u>							
From synthesis	155	19.4	20.9	-	-	-	-
As-spun fiber	151	6.7	7.2	0.90 ± 0.02	4.2 <sup>b</sup>	< 20 <sup>d</sup>	> 1000 <sup>d</sup>
Hot-drawn fiber	156	19.4	20.9	0.38 ± 0.01	6.2 <sup>c</sup>	184	240
<u>P(LL-co-CL-co-G)</u>							
From synthesis	151	22.3	24.0	-	-	-	-
As-spun fiber	137	15.1	16.2	0.76 ± 0.02	4.2 <sup>b</sup>	< 20 <sup>d</sup>	> 1000 <sup>d</sup>
Hot-drawn fiber	155	22.8	24.5	0.34 ± 0.01	6.2 <sup>c</sup>	181	114

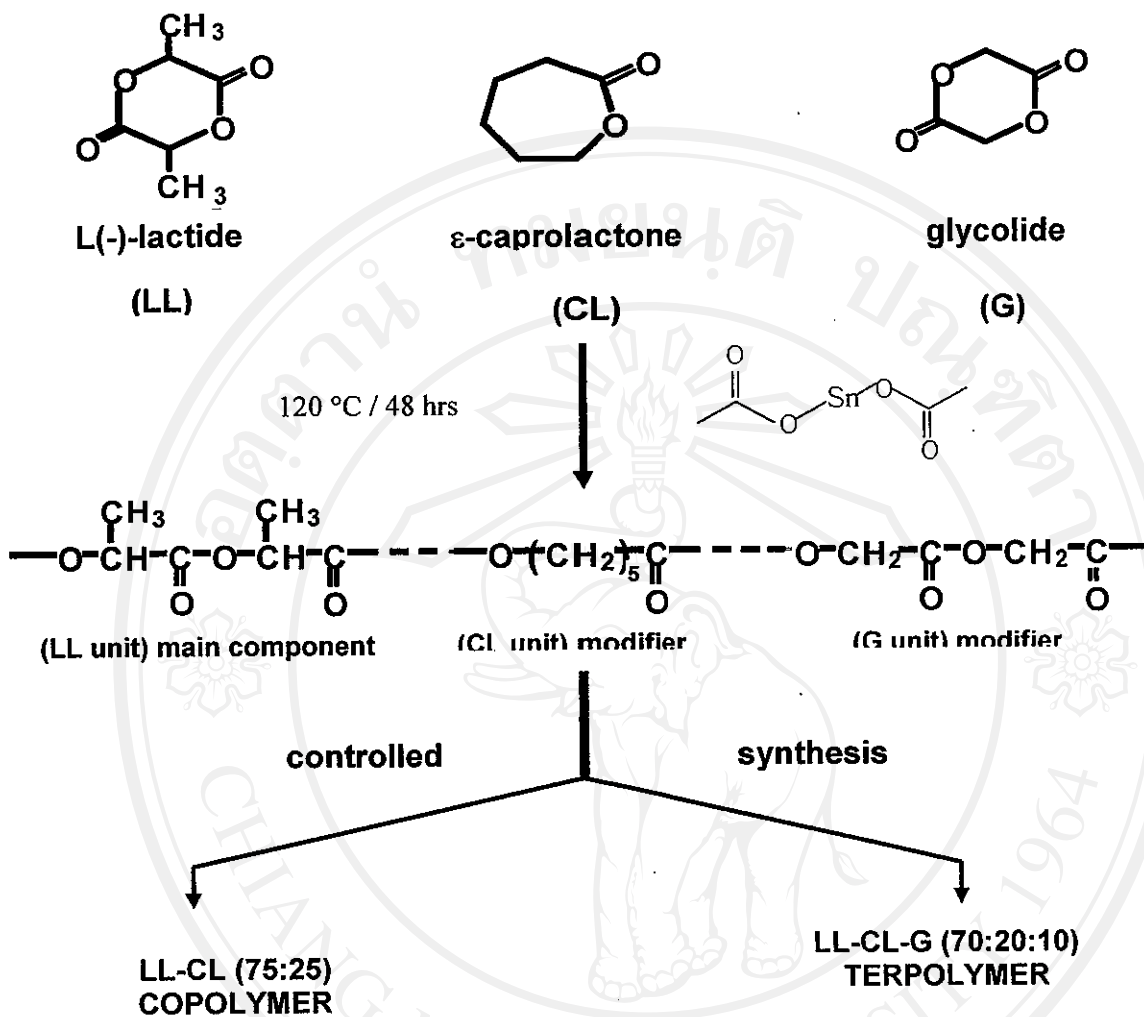
<sup>a</sup> as calculated from Eq. 2

<sup>b</sup> on-line draw ratio from melt spinning

<sup>c</sup> off-line draw ratio from hot-drawing

<sup>d</sup> as-spun fiber did not break within the limit of elongation of the testing machine

Table 3. Comparison of the effects of the processing steps on the thermal and mechanical properties of the P(LL-co-CL) copolymer and the P(LL-co-CL-co-G) terpolymer.



ลิขสิทธิ์มหาวิทยาลัยเชียงใหม่

Copyright© by Chiang Mai University

All rights reserved

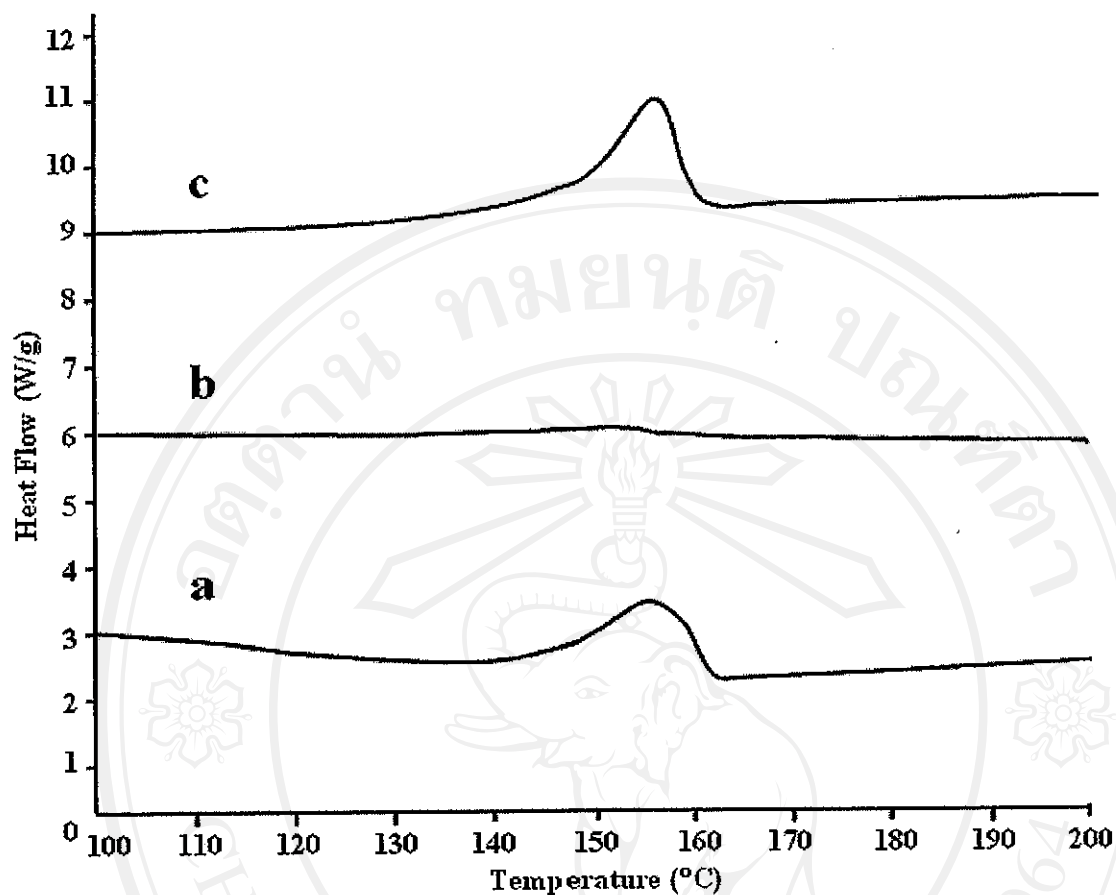


Fig. 2. DSC thermograms of the P(LL-co-CL) copolymer (heating rate = 10 °C/min;  $N_2$  atmosphere): (a) as synthesized, (b) as-spun fiber, (c) fiber after hot-drawing.

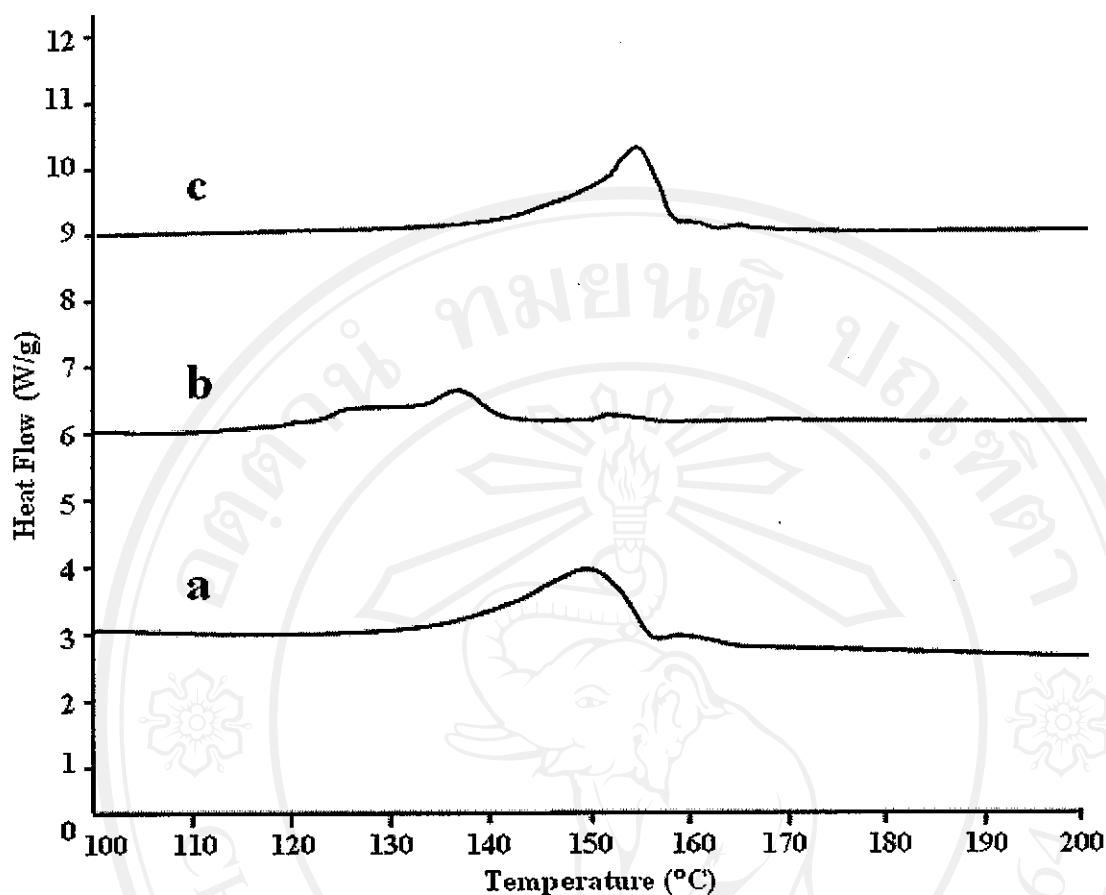


Fig. 3. DSC thermograms of the P(LL-co-CL-co-G) terpolymer (heating rate = 10 °C/min;  $N_2$  atmosphere): (a) as synthesized, (b) as-spun fiber, (c) fiber after hot-drawing.

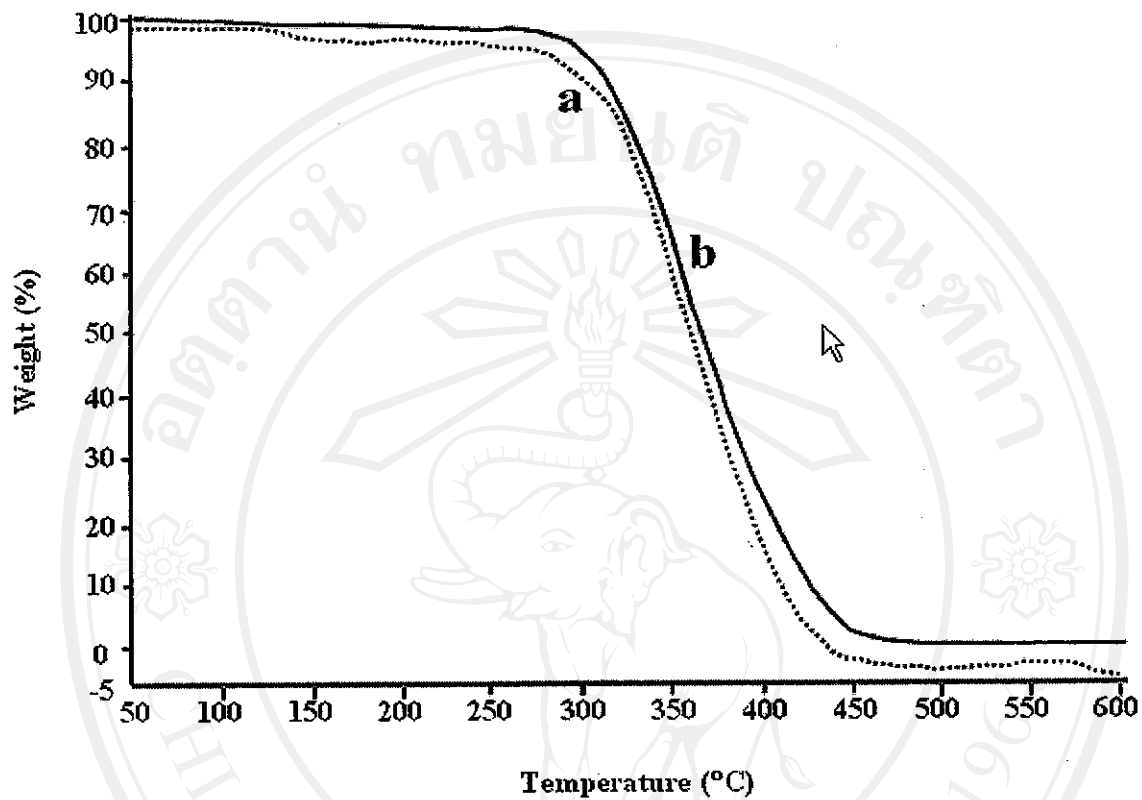


Fig. 4. TGA curves of the (a)  $P(LL\text{-}co\text{-}CL\text{-}co\text{-}G)$  terpolymer and (b)  $P(LL\text{-}co\text{-}CL)$

copolymer (heating rate = 20 °C/min;  $N_2$  atmosphere).

ลิขสิทธิ์มหาวิทยาลัยเชียงใหม่  
Copyright© by Chiang Mai University  
All rights reserved

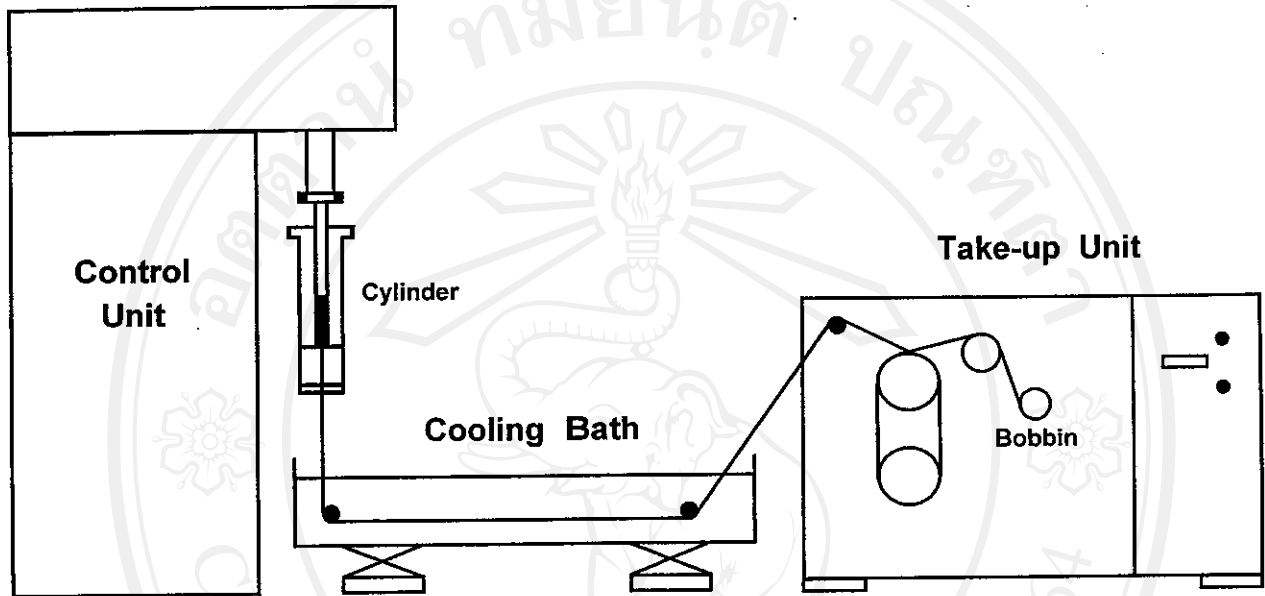


Fig. 5. Schematic arrangement of the small-scale melt spinning apparatus.

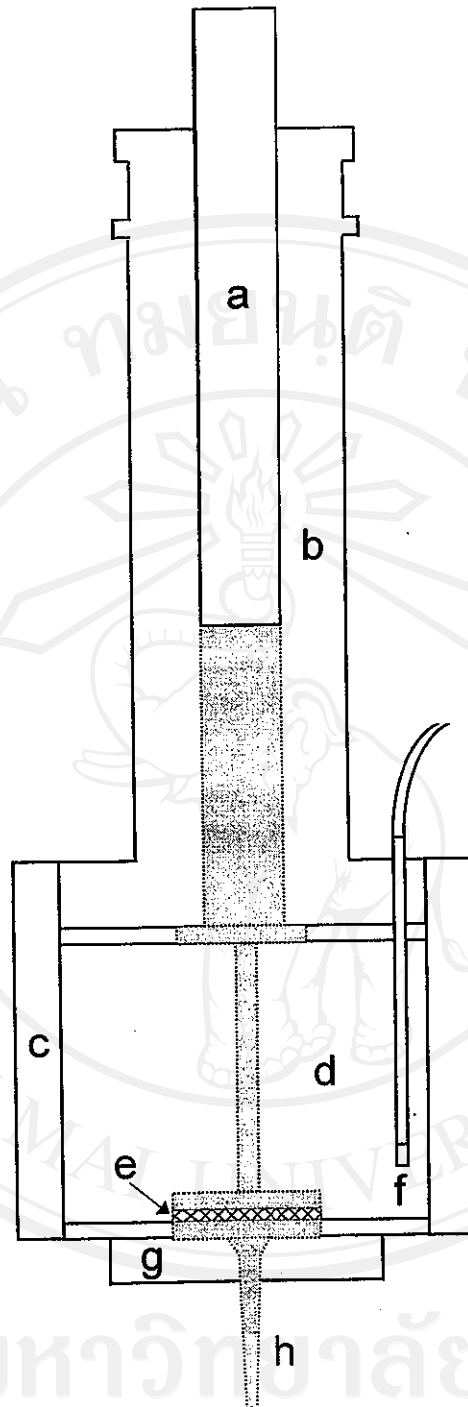


Fig. 6. Schematic diagram of the compression, melting and metering zones showing the (a) ram, (b) cylinder, (c) band heater, (d) heating block, (e) stainless steel filter mesh, (f) thermocouple, (g) spinnerette, and (h) extruded monofilament fiber.

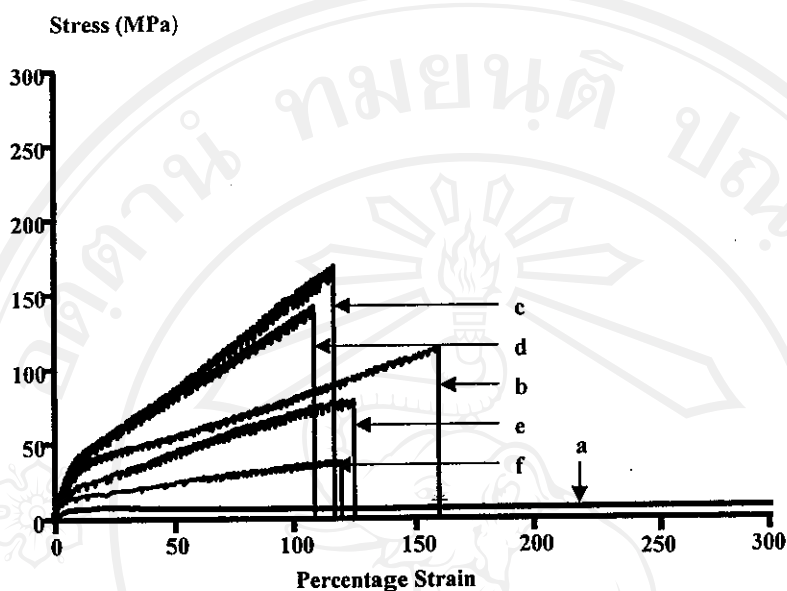


Fig. 7. Stress-strain curves for the P(LL-co-CL-co-G) terpolymer (a) as-spun, and after being hot-drawn at (b) 40 °C, (c) 50 °C, (d) 60 °C, (e) 70 °C and (f) 80

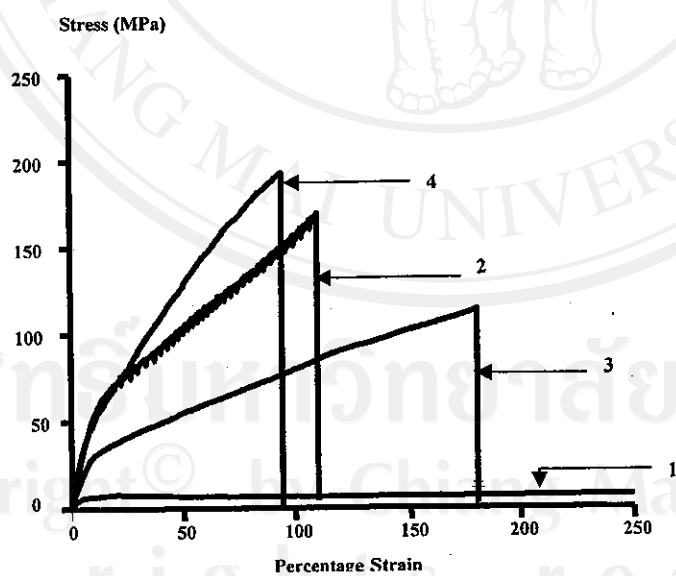


Fig. 8. Stress-strain curves for the P(LL-co-CL-co-G) terpolymer at various stages of its processing; in sequence: (1) as-spun, (2) after 1st hot-drawing at 50 °C, (3) after annealing at 60 °C and (4) after 2nd hot-drawing at 50 °C.



## ประวัติผู้เขียน

ชื่อ นางสาวสุภาพ บุญเกิด

วัน เดือน ปีเกิด 13 ธันวาคม 2524

ประวัติการศึกษา สำเร็จการศึกษาระดับมัธยมศึกษาตอนปลาย  
โรงเรียนอุดรพิชัยรักษ์พิทยา จังหวัดอุดรธานี ปีการศึกษา 2542

สำเร็จการศึกษาระดับปริญญาตรี  
มหาวิทยาลัยแม่โจ้ จังหวัดเชียงใหม่ ปีการศึกษา 2546

ที่อยู่ปัจจุบัน 27 หมู่ 6 ต. นาดี อ.เมือง จ. อุดรธานี 41000  
โทร. 042-201126 หรือ 085-0041446  
อีเมลล์ [nitro\\_o@hotmail.com](mailto:nitro_o@hotmail.com)

ลิขสิทธิ์มหาวิทยาลัยเชียงใหม่  
Copyright© by Chiang Mai University  
All rights reserved